Critical fluctuations in a binary mixture of polyethylene glycol and polypropylene glycol studied by ultrasonic and light scattering experiments

W. Mayer,[1] S. Hoffmann,[1] G. Meier,[2] and I. Alig[1,*]
[1]*Deutsches Kunststoff-Institut, 64289 Darmstadt, Schloβgartenstraβe 6, Germany;*
[2]*Max-Planck-Institut für Polymerforschung, Postfach 3148, 55021 Mainz, Germany*
(Received 9 September 1996)

The critical mixture of polypropylene glycol ($M=1000$ g/mol) and polyethylene glycol ($M=400$ g/mol) is investigated by light scattering and ultrasonic experiments in the homogeneous one-phase region (explored temperature and frequency range of the ultrasonic experiment are 0.1 K$\leqslant T-T_C \leqslant$21.3 K and 0.4 MHz$\leqslant f \leqslant$30 MHz; T_C is the critical temperature). The composition of the critical mixture was determined by measuring the volume ratios of the separated phases in the inhomogeneous two-phase region (criterion of equal volumes). The ultrasonic measurements are interpreted by a dynamic scaling theory for low molecular weight binary critical mixtures of Bhattacharjee and Ferrell. The characteristic time scale of the dynamics of the critical concentration fluctuations is described by the frequency $\omega_C=2D/\xi^2$ (D is the mutual diffusion coefficient and ξ the correlation length), which can also be expressed by $\omega_C=\omega_0\varepsilon^{z\nu}$ [$\varepsilon=(T-T_C)/T_C$ is the reduced temperature; ω_0 is the critical amplitude and $z\nu$ is the critical exponent]. The experimental values are $\omega_0=22.2$ MHz from light scattering experiments and $\omega_0=30$ MHz from ultrasonic data (within the frame of the Bhattacharjee-Ferrell theory). The low mutual diffusion coefficient of the mixture ($D=D_0\varepsilon^{-\nu^*}$, ν^* is the critical exponent; D_0 is the critical amplitude, with the experimental value from dynamic light scattering $D_0=4.0\times10^{-8}$ cm^2 s^{-1}) allows us to study the high frequency behavior of critical ultrasound attenuation in the range $10<\Omega<10^6$ ($\Omega=\omega/\omega_C$ is the reduced frequency; ω is the angular frequency of the measurement). The data follow the dynamical scaling theory well. [S1063-651X(97)03703-3]

PACS number(s): 36.20.−r

I. INTRODUCTION

The study of ultrasonic absorption and dispersion is an important tool for investigating the dynamics of relaxation processes in condensed matter [1]. In this way, the ultrasonic behavior of critical fluids attracted considerable attention, both experimentally and theoretically [1–13]. The experimental data are explained by the coupling of the sound wave with critical order parameter fluctuations. In a binary mixture the following mechanism of ultrasound attenuation is widely accepted: Because of alternate adiabatic compression and expansion of the fluid the (local) temperature and the pressure dependent critical temperature will change. Due to the lagged response of the concentration fluctuations (Fourier components) energy is dissipated. Bhattacharjee and Ferrell introduced a coupling constant g, which reflects this physical picture [9,13]:

$$g=\rho c_p[dT_C/dP-(\partial T/\partial P)_S], \tag{1}$$

where dT_C/dP is the change of the critical temperature T_C with the pressure P along the critical line, S is the entropy, ρ is the density, and c_P is the heat capacity of the critical mixture at constant pressure.

The value of g is often unknown because all of the thermodynamic quantities in Eq. (1) are seldom available. The importance of the first term in square brackets, dT_C/dP, was not recognized in the early attempts to explain the experimental findings. An example of a mixture where the observed critical excess ultrasound attenuation is mainly attributed to the pressure dependence of the critical temperature of demixing is the mixture 2-butoxyethanol/water [experimental values: $dT_C/dP=43$ mK/bar, $(\partial T/\partial P)_s=6$ mK/bar [14]].

The time scale of the decay of critical concentration fluctuations is characterized by a frequency $\omega_C=2D/\xi^2$ (ξ is the correlation length of critical concentration fluctuations, D is the mutual diffusion coefficient). Two aspects will be interesting with respect to the polymeric mixture investigated in this work. (i) Polymeric compounds attenuate the sound wave by Rouse-Zimm-like modes (for references see [15]). The time scale of these processes overlaps with the time scale of critical fluctuations. (ii) Because of the low mutual diffusion coefficients of polymeric mixtures [16–18] these systems seem to be a good candidate to study the high frequency behavior ($\omega>\omega_C$, ω is the angular frequency of the measurement) of critical ultrasound attenuation. The ultrasound behavior in the high frequency regime was discussed in the past by theorists [13]. In this regime the theories seem to be very sensitive to the incorporated mode coupling terms [8].

The time scale of the critical dynamics of binary mixtures is characterized experimentally by the critical amplitude ω_0 of ω_C ($\omega_C=\omega_0\varepsilon^{z\nu}$, $\varepsilon=(T-T_C)/T_C$ is the reduced temperature, ω_0 is the critical amplitude, $z\nu$ is the critical exponent). Experimental values of ω_0 for low molecular components are found in the interval 1–50 GHz [3].

In this paper we report experimental studies of the ultrasonic attenuation in a critical binary polymeric mixture. The system is characterized in Sec. III A. Special interest lies in the high frequency behavior of critical ultrasound attenuation (Sec. III C). The light scattering data (Sec. III B) are mainly intended to obtain the critical amplitudes of the correlation

*Author to whom correspondence should be addressed.

length ξ and the diffusion coefficient D to support the conclusions drawn from the ultrasonic measurements.

II. EXPERIMENT

A. Samples

The samples were commercial products by Merck (Darmstadt). Their molecular weight distribution was characterized by MALDI mass spectrometry (for polypropylene glycol, M_W=1000 g/mol, M_n=970 g/mol, M_W/M_n=1.03; for polyethylene glycol, M_W=406 g/mol, M_n=384 g/mol, M_W/M_n=1.06). Before mixing by weight, the probes were dried for several days in vacuum at 50 °C.

B. Light scattering

Light scattering experiments were performed with a commercial photometer (ALV, Langen). The light source was a He-Ne laser (Spectra-Physics, model 127) with 35 mW laser power. The goniometer covers an angular range $30°<\Theta<140°$, where Θ is the scattering angle. The incident and scattered laser beam were polarized perpendicular to the scattering plane (VV geometry). The dynamic light scattering experiments were performed with a correlator model ALV 5000/E. The temperature was controlled with an external thermostat with accuracy ±0.05 K. Static and dynamic light scattering experiments were carried out in the temperature interval $0.07\ \mathrm{K}\leqslant T-T_C\leqslant 1.42\ \mathrm{K}$ (corresponding to $2.3\times10^{-4}<\varepsilon<4.6\times10^{-3}$; ε is the reduced temperature). The transmitted light was measured with a photodiode.

C. Ultrasound

The ultrasonic absorption was measured by a resonator method (frequency range: $0.4\ \mathrm{MHz}<f<1.5\ \mathrm{MHz}$) and with the same resonator cell by a pulse transmission technique (frequency range: $6\ \mathrm{MHz}<f<30\ \mathrm{MHz}$) similar to the method described by Eggers and Funck [19]. The temperature was controlled with an external thermostat with accuracy 0.02 K. To avoid humidity the ultrasonic cell was held in a dry box filled with silica gel. This seemed to be necessary because the studied substances are hygroscopic. The measurements were carried out in a temperature range $0.1\ \mathrm{K}<T-T_C<21.3\ \mathrm{K}$, where T_C is the phase separation temperature of the critical mixture. Because of this wide range of temperature the cell alignment was checked carefully after the measurement.

III. RESULTS

A. Phase diagram

Figure 1 shows the measured cloud point curve of the polyethylene glycol (PEG)–polypropylene glycol (PPG) mixture. The cloud points were determined by cooling the mixture until it became turbid (cooling rate 1 mK/min). The measured cloud points of mixtures with compositions $y_{\mathrm{PPG}}<0.3$ (y_{PPG} is the mass fraction of PPG in the mixture) are shown in Fig. 1 with a dotted line because no sharp cloud point could be observed with the optical method.

To determine the composition of the critical mixture we studied the volume ratios of the phase separated samples (Fig. 2). The critical mixture is characterized by the criterion

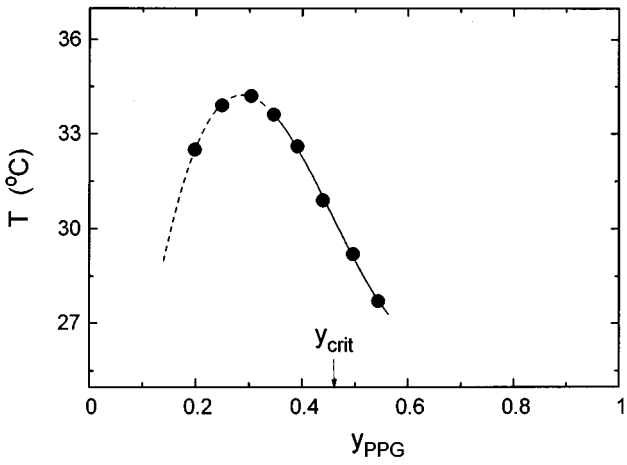

FIG. 1. Phase diagram of polyethylene glycol (M_W=400 g/mol)–polypropylene glycol (M_W=1000 g/mol). T is temperature. y_{PPG} is mass fraction of polypropylene glycol in the mixture. y_{crit} is the mass fraction of PPG of the critical composition.

of equal volumes in the vicinity of its phase separation temperature. From this, the mixture with mass fraction y_{PPG}=0.46 was selected. To this composition corresponds the phase separation temperature T_C=30.5 °C. We call it the critical temperature.

Inspection of the phase diagram (Fig. 1) shows that in contrast to binary mixtures the critical mixture does not coincide with the mixture that has the highest phase separation temperature. This finding is explained by the polydispersity of the oligomeric compounds [20]. All measurements reported in this study were performed with mixtures of composition y_{PPG}=0.46 (critical composition).

B. Light scattering

1. Static light scattering

In the vicinity of the critical point of demixing, the scattered light intensity mainly results from fluctuations of the

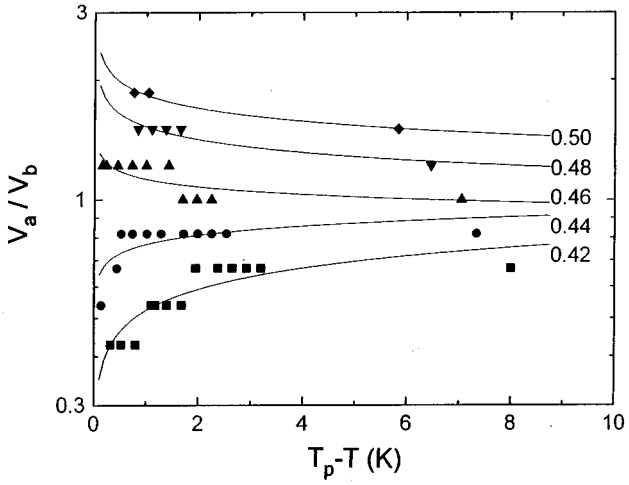

FIG. 2. Volume ratio of phase separated mixtures in the two-phase region. V_b is the volume of the upper phase, V_a is the volume of the lower phase. T_p is the phase separation temperature. The various values given in the picture correspond to different mass fractions of PPG.

concentration. This allows the determination of the structure function $S(k)=\langle|c(k)|^2\rangle$ by measuring the scattered intensity at different scattering angles, k is the absolute value of the wave vector and $c(k)$ is the Fourier component of the concentration fluctuation; k is related to the scattering angle Θ by $k=(4\pi n/\lambda)\sin(\Theta/2)$, n is the refractive index of the mixture, and λ is the wavelength of incident light. The structure function $S(k)$ is related to the scattered light intensity $I(k)$ by (see [16])

$$S(k)=\frac{I(k)\lambda^4\overline{\rho N}_L R_{\mathrm{VV}}^{\mathrm{ref}}}{I_{\mathrm{ref}}n_{\mathrm{ref}}^2 4\pi^2(n_A-n_B)^2\overline{M}_{\mathrm{mon}}}, \tag{2}$$

where the index ref means reference sample (here we used toluene); $\overline{\rho}$ is the mean density, M_{mon} is the mean molecular mass of the monomer units of A and B; n_A, n_B are the refractive indices of components A and B; and $R_{\mathrm{VV}}^{\mathrm{ref}}$ is the Rayleigh ratio of the reference sample.

In Eq. (2) single scattering is assumed. This seems appropriate in the explored temperature and scattering angle range, because the two compounds have similar refractive indices ($n_{\mathrm{PPG}}^D=1.450$, $n_{\mathrm{PEG}}^D=1.467$, $T=20$ °C).

It is convenient to describe the structure function by

$$S(k)=Ak_BT\chi(T)g(k\xi), \tag{3}$$

where A is the temperature independent constant, k_B is the Boltzmann constant, $\chi(T)$ is the osmotic compressibility at the temperature T ($\chi=\chi_0\varepsilon^{-\gamma}$, χ_0 is the critical amplitude, γ is the critical exponent), ξ is the correlation length of the critical order parameter fluctuations ($\xi=\xi_0\varepsilon^{-\nu}$, ξ_0 is the critical amplitude, ν is the critical exponent), and $\varepsilon=(T-T_C)/T_C$ is the reduced temperature. $g(x)$ is the Ornstein-Zernicke scaling function

$$g(x)=\frac{1}{1+x^2}. \tag{4}$$

Fisher proposed an improved scaling function $g_f(x)=1/(1+x^2)^{(1-\eta/2)}$, where η is a critical exponent (theoretical value $\eta=0.037$) [21]. In the explored temperature range we find it convenient to use the Ornstein-Zernicke form (4).

We shall add here a note concerning the definition of the reduced temperature ε. Usually, for polymeric mixtures ε is defined by $\varepsilon=(T-T_C)/T$ because the Flory-Huggins parameter χ_{FH} is related to the temperature by $\chi_{\mathrm{FH}}\propto 1/T$ [16]. However, we have estimated the Ginzburg number Gi on the basis of the crossover formalism [23] to be Gi$\cong$0.07, which means $\varepsilon\ll$Gi for the explored temperature range and hence different definitions of ε are inconsequential.

Figure 3 shows a plot of the inverse of the Rayleigh ratio of the scattered light intensity as a function of k^2 at different temperatures. The data fit the Ornstein-Zernicke form well. The slopes of the $1/R_{\mathrm{VV}}$ vs k^2 curves are constant within the experimental error limit. From the Ornstein-Zernicke plot we get with the relations (2)–(4) ξ as a function of the reduced temperature ε (Fig. 4). The data are fitted to the exponential law $\xi=\xi_0\varepsilon^{-\nu}$ by setting the theoretical $\nu=0.63$ [three dimensional (3D) Ising value] as a fixed value. Theoretical and experimental studies (on more symmetric) low molecular weight and polymeric binary mixtures confirm the validity of the 3D Ising behavior in a wide temperature region [17,18,22–24]. We get as a result of the fitting procedure $T_C=23.33$ °C, which coincides with the measured T_C within the experimental error limits. The critical amplitude is determined as $\xi_0=(0.60\pm0.01)$ nm. According to Sariban and Binder [25] the N dependence of ξ_0 in the 3D Ising limit is given by $\xi_0\propto N^{1-\nu}$, which was proven to be valid for a series of different polymer blends [24]. The blend under study has a mean value $\langle N\rangle=12.4$, which follows with $\xi_0=0.6$ nm exactly the cited prediction. The value for Γ^+, the amplitude for the susceptibility, scales, again according to [25], by $\Gamma^+\propto N^{2-\gamma}$. The experiment gives $\Gamma^+=15$, which is about a factor of 5 less than expected. We have no explanation as yet.

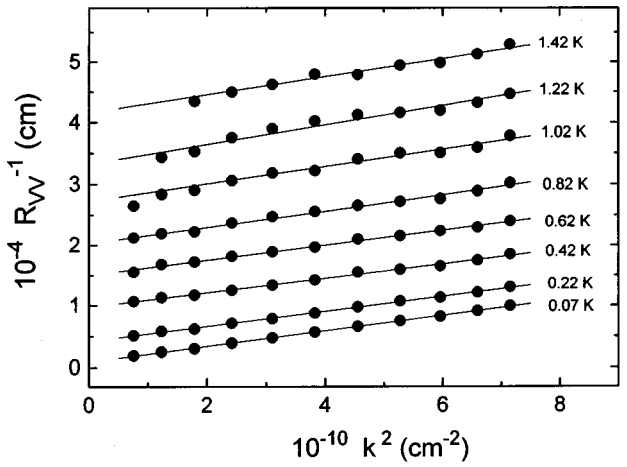

FIG. 3. $1/R_{\mathrm{VV}}$ as a function of k^2 at different values of $T-T_C$ as is indicated in the picture. R_{VV} is the Rayleigh ratio, k is the absolute value of the wave vector.

The value $T_C=23.33$ °C differs considerably from the experimental findings from cloud point measurements shown in Fig. 1 ($T_C=30.5$ °C) and that from ultrasonic measurements ($T_C=28.7$ °C). It should be noted here that the value of T_C is very sensitive to impurities, especially to water. In contrast to the light scattering cell the ultrasonic resonator could not

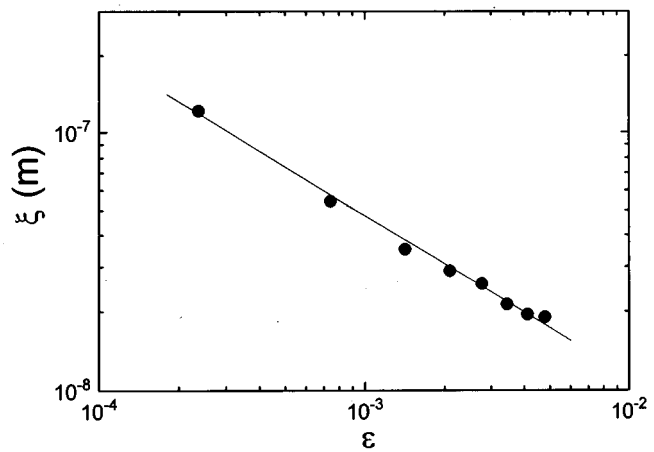

FIG. 4. Correlation length of critical concentration fluctuations ξ as a function of the reduced temperature ε. The solid line is given by $\xi=(0.6\times10^{-9})\varepsilon^{-0.63}$.

be completely closed. Therefore, the differences in T_C may be explained by different water absorption from the air. It was found in a separate experiment that addition of water led to an increase of the phase transition temperatures without considerable changes in the shape of the cloud point curves.

2. Dynamic light scattering

By measuring the autocorrelation function $S(k,t)$ of the scattered light intensity the decay of the order parameter can be obtained:

$$S(k,t)=\langle c(k,t)c(-k,0)\rangle. \tag{5}$$

It is described by a single exponential law [26]

$$S(k,t)=S(k)\exp[-\Gamma(k)t]. \tag{6}$$

The decay rate Γ is given by

$$\Gamma(k)=Dk^2, \tag{7}$$

$$D=\frac{L}{\chi(k)}. \tag{8}$$

In this expression $\chi(k)$ is the wave vector dependent osmotic compressibility and L a mobility (Onsager coefficient). In modern theory, the decay of concentration fluctuations couples to the transverse local momentum fluctuations. This yields a wave vector dependent mobility $L(k)$. The measured decay rate contains, besides the critical part, a noncritical background. This situation is commonly described by a splitting of L into a background term L_B, which is assumed as a constant, and the critical term L_C, $L=L_B+L_C$ [27,28]. This gives the following relations for the measured diffusion coefficient D_M [defined by Eq. (7)]:

$$D_M=D_B+D_C, \tag{9}$$

$$D_B=L_B/\chi(k), \tag{9a}$$

$$D_C=L_C(k)/\chi(k). \tag{9b}$$

D_C is given by the theory as follows [29–31]:

$$D_C=R\,\frac{k_BT}{6\pi\eta\xi}\,\Omega(k\xi). \tag{10}$$

The shear viscosity η can be expressed by [32]

$$\eta=\eta_B(Q_0\xi)^{x_\eta}, \tag{11}$$

where η_B is the background viscosity, Q_0 is the microscopic cutoff wave number, x_η is the critical exponent, and R is a universal dynamic amplitude ratio.

The scaling function $\Omega(x)$ is given by Burstyn *et al.* [31]:

$$\Omega(x)=\Omega_K(x)[S(x)]^{x_\eta}, \tag{12}$$

$$\Omega_K(x)=(3/4x^2)[1+x^2+(x^3-x^{-1})\arctan x], \tag{13}$$

where Ω_K is the Kawasaki function, $\Omega_K(x)\cong 1+\frac{3}{5}x^2$ for $x\ll 1$, and

$$S(x)=a(1+b^2x^2)^{1/2}, \tag{14}$$

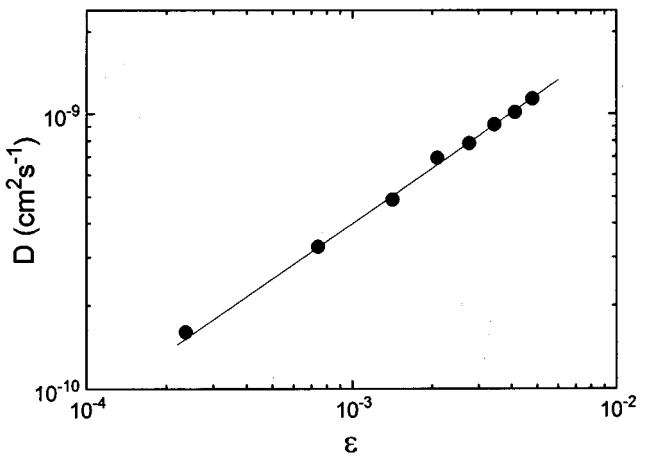

FIG. 5. Mutual diffusion coefficient D as a function of the reduced temperature ε. The solid line is given by $D=(4.0\times10^{-8})\varepsilon^{0.664}$ with $T_c=23.33$ °C.

where a and b are constants.

To describe the experimental data we will use the relations (7)–(14) in the following form:

$$D_M=D\Omega_K(k\xi), \tag{15}$$

$$D=D_0\varepsilon^{\nu^*}, \tag{16}$$

with $\nu^*=\nu(1+x_\eta)$ the critical exponent.

We assume $S(x)=1$, which is an appropriate approximation in the measured range $0.2<x<3$, $x=k\xi$. Further, we neglect the background diffusion term, which has been shown to be small in most systems not too far away from the critical solution temperature or not too close at the critical solution temperature [16,31]. A proper discussion of it in the explored system would make it necessary to measure the shear viscosity of the mixture [27,32]. We have no such data.

The diffusion coefficient D was determined by extrapolation of $[\Gamma/k^2]$ to zero wave vector in the limit $k\xi\ll 1$: $D=\lim(k\to 0)[\Gamma/k^2]$, see Eq. (13). Then Fig. 5 is obtained. The solid line in Fig. 5 was obtained by a fit to the data according to the exponential law $D=D_0\varepsilon^{-\nu^*}$ by setting the critical exponent to the fixed value $\nu^*=0.664$ [$\nu^*=\nu(1+x_\eta)$, $x_\eta=0.054$ is the theoretical value from a mode coupling approach [33]]. From the fit using $T_C=23.33$ °C obtained from static light scattering (see above) we get $D_0=(4.0\pm0.1)10^{-8}$ cm^2 s^{-1}.

In Fig. 6 the scaling property of the data points is demonstrated. The solid line is calculated with relation (13).

It should be noted that the data points are not good enough to decide if $\nu=0.63$ and $\nu^*=0.664$ are the proper exponents to describe the static and dynamic light scattering data. Alternatively, we can ask if the Kawasaki scaling is appropriate. It is known that multicomponent systems can show so-called renormalized exponents which differ from the values for binary mixtures, see, e.g., [34]. We hope to clarify this point in a later study by supporting the experimental equipment with a better temperature control. Because the light scattering data are mainly intended to support the ultrasonic experiment, we think that the results of this section are satisfactory.

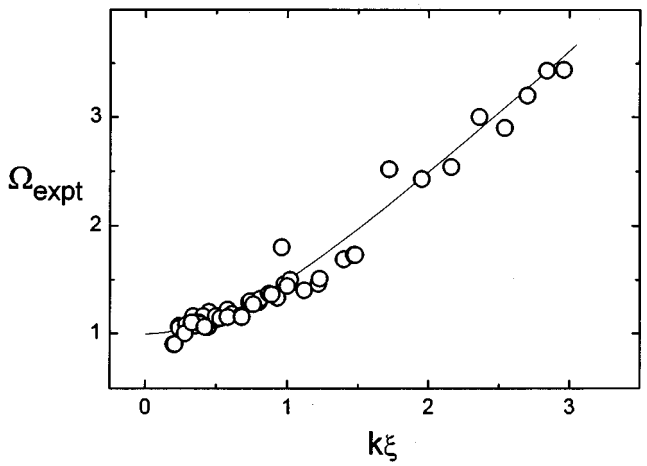

FIG. 6. Ω_{expt} as a function of $k\xi$. $\Omega_{expt}=\Gamma/(DK^2)$, Γ is the measured linewidth, $D=D_0\varepsilon^{-\nu^*}$, $D_0=4.0\times10^{-8}$ cm^2 s^{-1}. The solid line is calculated with the Kawasaki scaling function (13).

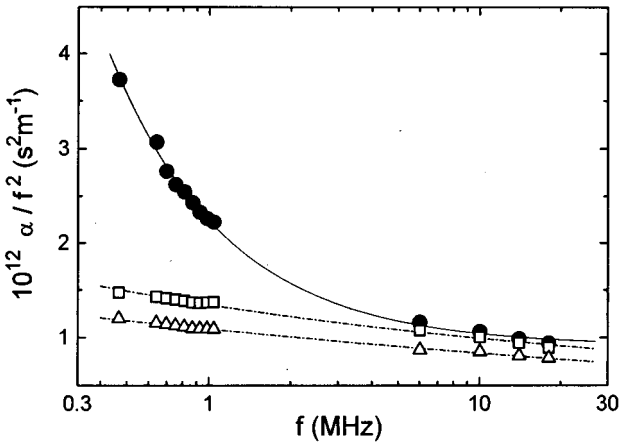

FIG. 8. α/f^2 as a function of the frequency. ●, measured α/f^2 from the mixture; □, linear background; △, reciprocal background. $T=28.9$ °C.

We are now able to calculate the amplitude of the characteristic frequency of the order parameter decay $\omega_0=2D_0/\xi_0^2$. With $\xi_0=0.6$ nm and $D_0=4.0\times10^{-8}$ cm^2 s^{-1} we get $\omega_0=22.2$ MHz.

C. Ultrasound

1. Experimental findings

In a classical fluid a propagating sound wave is attenuated by the mechanism of viscous damping and thermal conduction. The attenuation coefficient α [(length)$^{-1}$] behaves as $\alpha\propto f^2$, where f is the frequency (Kirchhoff-Stokes law, see, e.g., [35]). In a polymeric system other processes contribute to the observed ultrasound attenuation. An important mechanism of sound attenuation in these systems is the delayed response of Rouse-Zimm-like modes, which yields $\alpha\propto f^{2-n}$ [$n=-\frac{1}{2}$ (Rouse); $n=-\frac{1}{3}$ (Zimm)] (for references see, e.g., [15]). Figure 7 shows measured attenuation α/f^2 of the pure components and the critical mixture at two different temperatures. The attenuation of the lower molecular PEG component behaves like a classical fluid in the frequency range considered, the PPG absorption shows a Rouse-Zimm-like behavior. The mixture shows an excess attenuation, which behaves significantly differently. The excess attenuation is only weakly temperature dependent.

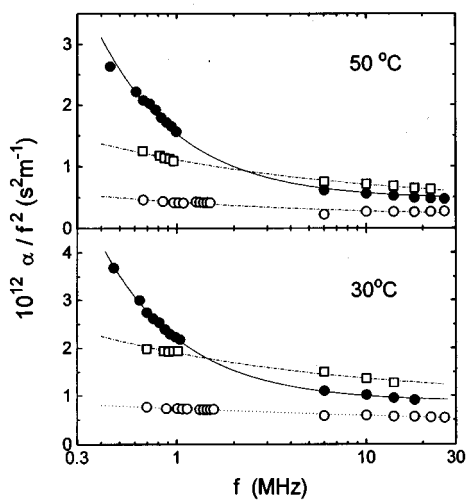

FIG. 7. α/f^2 as a function of the frequency f at the temperatures $T=50$ °C and $T=30$ °C. ●, experimental data from the mixture; ○, experimental data from pure PEG; □, experimental data from pure PPG.

To get further physical insight into the mixture behavior we must separate the effect of the mixture (we will interpret it as a critical ultrasound contribution) from the background effect of the pure components. Because no theoretical way to determine the background contribution exists we tried two procedures for background estimation. The basic assumption is an additive contribution of the mixture and the background to the observed α/f^2, $\alpha/f^2=(\alpha/f^2)_{\rm mix}+(\alpha/f^2)_b$ (the indices mix and b stand for mixture and background, respectively). The background terms are built as follows: Arithmetical mean background $(\alpha/f^2)b=\phi(\alpha/f^2)_{\rm PPG}+(1-\phi)(\alpha/f^2)_{\rm PEG}$ or reciprocal mean background $(\alpha/f^2)_b^{-1}=\phi(\alpha/f^2)_{\rm PPG}^{-1}+1(-\phi)(\alpha/f^2)_{\rm PEG}^{-1}$, where ϕ is the volume fraction of PPG in the mixture. The reciprocal construction was motivated by shear viscosity data in a polymeric mixture [16]. Figure 8 shows experimental data of a mixture in the vicinity of the phase separation temperature together with the two background constructions. In the subsequent sections we will use only the reciprocal background because mixture data points corrected with it will give slightly better fittings to theoretical models of critical ultrasound attenuation. It should be noted that this difference is not significant, though.

2. Critical ultrasound absorption

In the following, we will characterize the ultrasonic measurements by critical ultrasound theories for low molecular weight binary liquid mixtures. This is mainly motivated by the light scattering results, which show the presence of critical concentration fluctuations. The light scattering data can properly be described by common laws of static and dynamic critical phenomena well established for binary liquid mixtures.

Critical ultrasound attenuation is founded in the lagged response of the critical concentration fluctuations to the pres-

sure induced temperature variations dT_C/dP (pressure dependence of the critical temperature along the critical line) and $(\partial T/\partial P)_S$ (adiabatic temperature rise). Both effects are incorporated in the coupling constant g defined by $g=\rho c_P[dT_C/dP-(\partial T/\partial P)_S]$, see Eq. (1). To gain some insight into the physical mechanism of critical ultrasound attenuation of the PEG-PPG blend, we measured the temperature coefficient dT_C/dP of the critical mixture polyethylene glycol (M_w=600 g/mol)–polypropylene glycol (M_w=1000 g/mol). The measurement gave the following result: $dT_C/dP=-4\pm2$ mK/bar. We plan to present a full discussion of this experiment in a later work [37]. Experimental values of the adiabatic temperature rise $(\partial T/\partial P)_S$ of the critical mixture are not available. With the thermodynamic relation $(\partial T/\partial P)_S=T\alpha_{P,Xc}/(\rho_C c_{P,Xc})$ ($\alpha_{P,Xc}$ is the thermal expansion coefficient of the critical mixture, ρ_C is the density of the critical mixture, $c_{P,Xc}$ is heat capacity, and T is temperature) and the values $\rho_C=1.09$ g cm^{-3} (mean value of the densities of the pure samples at $T=302$ K), $c_{P,Xc}=0.49$ cal g^{-1} K^{-1} (c_P of PEG 750 at 306.6 K taken from [38]), $\alpha_{P,Xc}=0.71\times10^{-3}$ K^{-1} (mean value of the thermal expansion coefficient of the pure samples at $T=302$ K), and $T=302$ K we get as a crude estimate $(\partial T/\partial P)_S=9.6$ mK/bar. With these values the coupling constant g is estimated by $g=-0.30$.

Theoretical studies of critical ultrasound behavior are based on calculations of the frequency dependent complex bulk viscosity [7,8,10] or the frequency dependent complex specific heat [9,11,12].

To be specific, we will compare the measurements with results of the dynamic scaling theory of Bhattacharjee and Ferrell [9], which was very successful by describing experimental data of low molecular weight components, especially in the high frequency limit [2,3]. In this limit the dynamic renormalization group study of Kroll and Ruhland gives similar results [10].

A dynamic scaling argument for the complex heat capacity leads to a simple functional dependence of the attenuation α/f^2 from frequency at the critical solution point

$$(\alpha/f^2)_c=Kf^{-[1+\alpha/(z\nu)]}+B, \tag{17}$$

where $\alpha=0.11$ is the critical exponent of the specific heat of the critical mixture at constant pressure, $\nu=0.63$ is the critical exponent of the correlation length ξ, $z=3(1+x_\eta)$, where $x_\eta=0.054$ is the critical exponent of the shear viscosity obtained from a mode coupling approach [31], and $\alpha/z\nu=0.057$. B is a phenomenologically added background term, not further specified (Kirchhoff-Stokes law). In our case B is identical to $(\alpha/f^2)_{b,c}$ at the critical point. K is a frequency independent constant.

In Fig. 9 the experimental data from a measurement at the vicinity of the critical solution temperature ($T-T_C=0.1$ K) are presented. Because α/f^2 shows only a weak temperature dependence it is appropriate to identify it as a measurement at the critical temperature. In the upper part (a), mixture data are presented together with the reciprocal background curve, calculated using the reciprocal background construction. In the lower part (b), the background data points are subtracted. It can be seen that the functional form of relation (17) is

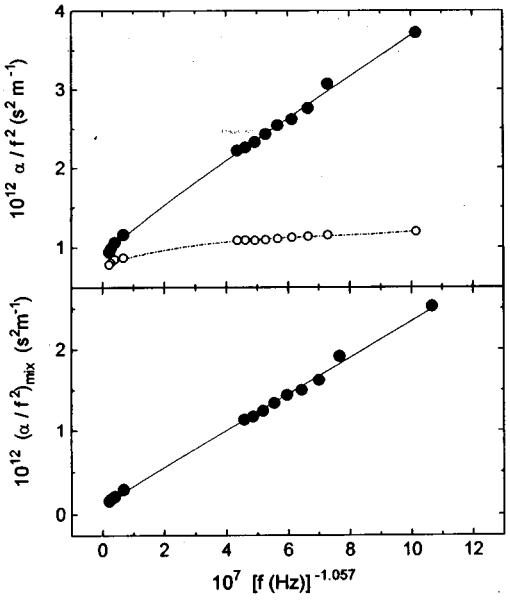

FIG. 9. (a) α/f^2 as a function of $f^{-1.057}$. ●, experimental data from the mixture; ○, reciprocal background $(\alpha/f^2)_B$. (b) $(\alpha/f^2)_{\rm mix}$ as a function of $f^{-1.057}$. $(\alpha/f^2)_{\rm mix}=(\alpha/f^2)-(\alpha/f^2)_B$. α/f^2 is the observed attenuation of the mixture. $T=28.9$ °C.

represented by the experimental data. From a linear fit to the data in Fig. 9(b) we get from the slope K the value of $A^*=Ku_c$, $A^*=3.66\times10^{-3}$ s$^{-1.057}$, where u_C is the ultrasound velocity at the critical temperature ($u_C=1509.4$ m/s). We will need it in the following. In contrast to Eq. (17) the experimental background is frequency dependent. The assumption that the critical and the background attenuation contribute additively to the observed attenuation seems appropriate.

To describe the critical ultrasound behavior in the whole frequency and temperature range, Bhattacharjee and Ferrell give a parameter free relation for the reduced quantity $(\alpha_\lambda/\alpha_{\lambda,C})$ (α_λ is the contribution to the attenuation coefficient per wavelength from critical order parameter fluctuations at a given temperature and $\alpha_{\lambda,C}$ is the contribution to the attenuation coefficient per wavelength from critical order parameter fluctuations at the critical temperature):

$$\alpha_\lambda/\alpha_{\lambda,c}=G(\Omega), \tag{18}$$

where $\Omega=\omega/\omega_C$ is the reduced frequency.

The authors give an approximated relation for the scaling function $G(\Omega)$,

$$G(\Omega)=[1+0.414(\Omega_{1/2}/\Omega)^{1/2}]^{-2}, \tag{19}$$

with $G(\Omega_{1/2})=\frac{1}{2}$, $\Omega_{1/2}\cong2.1$ [9].

This relation can directly be compared with the experimental findings. The only parameter which has to be known is the amplitude ω_0 of the characteristic frequency, which is available from light scattering experiments or can be determined by fitting the ultrasonic data (see below).

From Eqs. (18) and (19) we get the critical attenuation per wavelength as a function of the reduced temperature ε and the frequency ω:

$$\alpha_\lambda(\varepsilon,\omega)=2\pi AF(\Omega), \tag{20}$$

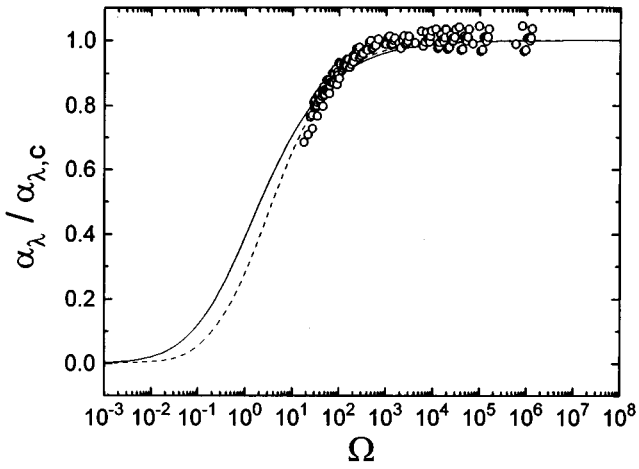

FIG. 10. $\alpha_\lambda/\alpha_{\lambda,C}$ as a function of the reduced frequency Ω. α_λ is the attenuation per wavelength, $\alpha_{\lambda,C}$ is the attenuation per wavelength at the critical temperature. The solid line was calculated with Eq. (19). The dotted line was calculated numerically with an integral representation of $G(\Omega)$ [9(b)].

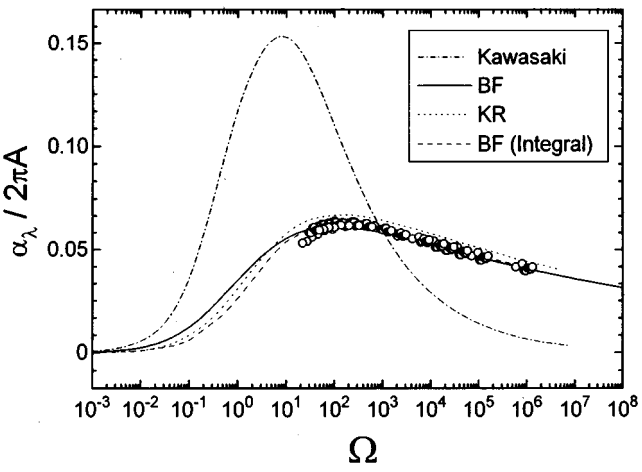

FIG. 11. $\alpha_\lambda/2\pi A$ as a function of the reduced frequency Ω [see Eq. (20)]. α_λ is the attenuation per wavelength. The solid line (BF) is calculated with Eq. (21). The experimental data are fitted to Eq. (20) (see text). The curve KR is calculated with $F(\Omega)=\mathrm{Im}[f(\overline{\nu})/f(0)]$ by setting $\Omega=\overline{\nu}/2$ (for definitions see Ref. [10]). The curve Kawasaki is calculated numerically with $F(\Omega)=\int_0^\infty (x^2/(1+x^2)^2\{\Omega K(x)/[K^2(x)+\Omega^2]\}dx$, see [7]. The curve BF (Integral) is calculated numerically with $F(\Omega)=\pi\alpha/(2z\nu)\Omega^{-\alpha/z\nu}((3/\pi)\int_0^\infty[x/(1+x)^2]\{[\Omega x(1+x)^{1/2}]/[x^2(1+x)+\Omega^2]\}dx)$.

$$F(\Omega)=(\pi\alpha/2z\nu)\Omega^{-\alpha/(z\nu)}G(\Omega). \tag{21}$$

From Eqs. (17), (20), and (21) follows $A=A_0\varepsilon^{-\alpha}$ with $A_0=(1/2\pi)(2z\nu/\pi\alpha)(2\pi/\omega_0)^{\alpha/z\nu}A^*$. With the fitting value of A^* and $\omega_0=22.2$ MHz we get $A_0=2.5\times10^{-3}$. As has been pointed out by Tanaka and Wada [13], the other theories of critical ultrasound attenuation mentioned here can be brought to the functional form (20). They differ mainly in the concrete expression of the scaling function $F(\Omega)$. The amplitude A can be approximately expressed by the common relation $A=A_0\varepsilon^{-\alpha}$ with $A_0=(u^2g^2c_{P,0})/(2T_Cc_P^2)$, where α is the critical exponent of the heat capacity of the critical mixture at constant pressure, u is the ultrasound velocity, g is the coupling constant, c_P is the heat capacity, and $c_{P,0}$ is the critical amplitude of the heat capacity. The explicit calculation of A would make it necessary to measure the heat capacity of the critical mixture in the vicinity of the critical temperature. No such data are available. On the assumption that the two-scale-factor-universality hypothesis is true for the studied polymeric mixture we get the value of the critical amplitude $c_{P,0}$ of the critical part of the heat capacity. The two-scale-factor-universality hypothesis asserts a relationship between the amplitude of the critical concentration fluctuations ξ_0 and $c_{P,0}$: $R_\xi=(\rho_C\alpha c_{P,0}/k_B)^{1/3}\xi_0$ (k_B is the Boltzmann constant, ρ_C is the density of the critical mixture, and α is the critical exponent of the specific heat, theoretical value $\alpha=0.11$). The value $R_\xi=0.27$ is given by a renormalization group study [39]. Using $\xi_0=0.6$ nm and the thermodynamic values quoted above we get $c_{P,0}=10.5$ J kg^{-1} K^{-1} and $A_0=8.5\times10^{-4}$. With respect to the crude assumptions made in the evaluation of A_0 this value seems to coincide with the experimental value $A_0=2.5\times10^{-4}$ obtained above from an analysis of Fig. 9.

Figure 10 shows $(\alpha_\lambda/\alpha_{\lambda,C})$ as a function of the reduced frequency Ω. The $(\alpha_\lambda/\alpha_{\lambda,C})$ values were drawn directly from experimental data after subtraction of the background contribution $(\alpha/f^2)_b$ and by identifying α_λ of the mixture at the vicinity of the critical solution temperature ($T-T_C=0.1$ K) with $\alpha_{\lambda,C}$. Because the experimental α_λ data show only a weak temperature dependence this setting seems appropriate. The value $\omega_0=30$ MHz was used to evaluate the reduced frequency Ω. It was determined by fitting the $(\alpha_\lambda/\alpha_{\lambda,C})$ values to the functional form given in Eqs. (18) and (19). The difference between this value of ω_0 and $\omega_0=22.2$ MHz obtained from light scattering data results presumably from different critical phase separation temperatures observed in these two experiments (T_C, light scattering: 23.33 °C; T_C, ultrasound: 28.8 °C). Because the viscosity is reduced at higher temperatures ω_0 of the ultrasound experiment has the greater value. In this way we think both experiments are in accordance.

Figure 11 shows the critical part of the attenuation per wavelength α_λ scaled with the parameter $2\pi A$ according to relation (20). The experimental data are fitted to the functional relations (19)–(21) as described above. These relations are presented in Fig. 11 by the solid line marked BF. In addition to this, predictions from an integral representation of the scaling function $F(\Omega)$ of Ferrell and Bhattacharjee [9(b)] [named BF (Integral)], a renormalization group study of Kroll and Ruhland [10], and an older mode coupling study of Kawasaki [7] (two-mode contribution, Ornstein-Zernicke correlation function; the four-mode contribution is studied in [8(b)]) are shown. Figure 11 shows that the experimental data are well represented by the theories of Kroll and Ruhland and Bhattacharjee and Ferrell. It should be recognized that the value of A must be used as a fit parameter.

To get further evidence for the assertion that critical concentration fluctuations are responsible for the observed excess attenuation we studied the temperature dependence of ω_C with the following relation which can be obtained from Eqs. (17)–(19):

$$(\alpha/f^2)_{\mathrm{expt}}=\frac{A^*}{u_T}f^{-1.057}\left(1+0.2393\frac{\sqrt{\omega_C}}{\sqrt{f}}\right)^{-2}+b_T. \tag{22}$$

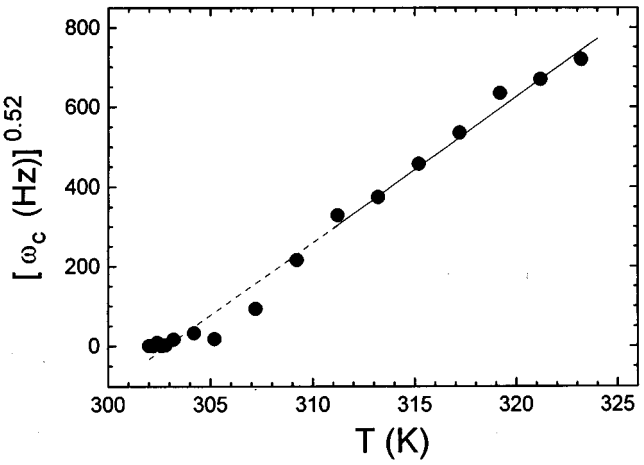

FIG. 12. $\omega_C^{0.52}$ vs temperature T. ω_C is the characteristic frequency obtained by a fitting to Eq. (22) (see text).

Here f is the frequency, $(\alpha/f^2)_{\text{expt}}$ the measured attenuation, u_T the temperature dependent ultrasound velocity, A^* see above, ω_C the characteristic frequency defined above, and b_T the background, which is here assumed to be frequency independent.

From a fit of the frequency dependence of the experimental $(\alpha/f^2)_{\text{expt}}$ data at different temperatures to relation (22) we get the characteristic frequency ω_C (fit parameter) as a function of the temperature. Figure 12 shows the result of this analysis. Because of $\omega_C=\omega_0\varepsilon^{z\nu}$, $1/z\nu=0.52$ (theoretical value, see above), we expect a linear relationship between $\omega_C^{0.52}$ and the temperature T. This is confirmed in Fig. 12 for temperatures $T>310$ K. For lower values of T the second term in the large parentheses of Eq. (22) is too low to allow a correct determination of ω_C. The solid line in Fig. 12 comes from a linear fit to the data with $T>311$ K. From this we obtain $T_C=28.62$ °C and $\omega_0=57$ MHz. The value of T_C agrees in the experimental error limits with the experimental value $T_C=28.7$ °C obtained in the ultrasonic experiment. The value of ω_0 is somewhat higher than the value $\omega_0=30$ MHz from ultrasonic data quoted above and $\omega_0=22.2$ MHz from light scattering data (see the comments made above).

IV. CONCLUSION

From our experimental data we draw the following conclusions.

(1) The measured excess ultrasonic attenuation of the critical mixture PEG 400–PPG 1000 can be attributed to the presence of critical concentration fluctuations.

(2) The data reproduce the high frequency regime of theoretical predictions of Bhattacharjee and Ferrell [9] and Kroll and Ruhland [10].

(3) Rouse-Zimm-like contributions of the pure components can be incorporated as an additive background term to the critical part of the ultrasound attenuation.

The present work extends former ultrasonic studies of critical mixtures of low molecular weight (see, e.g., [2,3], and references therein) and polymeric solutions [4,5] to polymeric melts. It seems that all these works confirm the common physical picture of critical ultrasound attenuation. One may think that the next step in critical ultrasonic experiments should be the study of higher molecular weight polymeric mixtures. The present work shows that the critical contribution of high molecular weight polymeric mixtures would give a nearly temperature independent contribution to the observed attenuation α_λ. Further, we would expect large contributions from other molecular processes like Rouse dynamics. In this way, oligomeric mixtures, like the system explored in this work, seem to be a good starting point for further investigations. Another interesting question is the behavior of Rouse modes in a critical medium. We think these difficult processes will attract considerable theoretical and experimental attention in the future. At present, we have only a crude understanding of them. For example, a mode coupling approach to this question from Genz and Vilgis [36] shows a critical slowing down of the first Rouse mode. In contrast, the self-diffusion coefficient remains nonsingular. Processes like this are expected to have an influence on the observed ultrasound attenuation. In this way, it would also be illuminating to study noncritical mixtures. The aim of such experimental studies could be the building of crossover functions: (i) The crossover from critical behavior to noncritical behavior by varying the composition; (ii) the crossover from common Rouse dynamics to critical screened Rouse dynamics.

ACKNOWLEDGMENTS

The authors wish to thank Dr. B. Steinhoff and L. Kühne for the measurement of the pressure dependent thermodynamic coefficients. We also thank K. Rode and R. Ghahary for characterization of the molecular weight distributions. The financial support of the Deutsche Forschungsgemeinschaft (Grant No. A1 93/1-1) and the Max-Planck Gesellschaft is gratefully acknowledged. I.A. wishes to thank Professor D. Woermann and Professor V. A. Solovyev for stimulating discussions.

[1] K. F. Herzfeld and T. A. Litovitz, *Absorption and Dispersion of Ultrasonic Waves* (Academic, New York, 1959).
[2] C. W. Garland and G. Sanchez, J. Chem. Phys. **79**, 3090 (1983); **79**, 3100 (1983).
[3] D. Woermann, Prog. Colloid Polymer. Sci. **84**, 165 (1991).
[4] L. A. Zubkov, Yu. S. Manucharov, S. A. Manucharova, and R. K. Turniyasov, Vysokomol. Soedin., Ser. A **29**, 1932 (1987).
[5] D. B. Fenner, J. Chem. Phys. **87**, 2377 (1987).
[6] U. Kaatze and U. Schreiber, Chem. Phys. Lett. **148**, 241 (1988).
[7] K. Kawasaki, Phys. Rev. A **1**, 1750 (1970).
[8] (a) Y. Shiwa and K. Kawasaki, Prog. Theor. Phys. **66**, 118 (1981); (b) **66**, 406 (1981).
[9] (a) J. K. Bhattacharjee and R. A. Ferrell, Phys. Rev. A **24**, 1643 (1981); (b) R. A. Ferrell and J. K. Bhattacharjee, *ibid*. **31**, 1788 (1985).

[10] D. M. Kroll and J. M. Ruhland, Phys. Rev. A **23**, 371 (1989).
[11] M. Fixman, J. Chem. Phys. **36**, 1961 (1962).
[12] L. Mistura, J. Chem. Phys. **57**, 2311 (1972).
[13] H. Tanaka and Y. Wada, Phys. Rev. A **32**, 512 (1985).
[14] M. Sieber and D. Woermann, Ber. Bunsenges. Phys. Chem. **95**, 15 (1991); C. Baaken, L. Belkoura, S. Fusenig, Th. Müller-Kirschbaum, and D. Woermann, *ibid*. **94**, 150 (1991).
[15] M. Schulz and I. Alig, J. Chem. Phys. **97**, 2772 (1992).
[16] G. Meier, W. Momper, and E. W. Fisher, J. Chem. Phys. **97**, 5884 (1992).
[17] W. Theobald and G. Meier, Phys. Rev. E **51**, 5776 (1995).
[18] H. Sato, N. Kuwahara, and K. Kubota, Phys. Rev. E **53**, 3854 (1995).
[19] F. Eggers and Th. Funck, Rev. Sci. Instrum. **44**, 969 (1973).
[20] R. Koningsveld, L. A. Kleintjens, and H. M. Schoffeleers, Pure Appl. Chem. **39**, 1 (1974).
[21] M. E. Fisher, J. Math. Phys. **5**, 944 (1964).
[22] M. A. Anisimov, S. B. Kiselev, J. V. Sengers, and S. Tang, Physica A **188**, 487 (1992).
[23] M. Y. Belyakov and S. B. Kiselev, Physica A **190**, 75 (1992).
[24] D. Schwahn, G. Meier, K. Mortensen, and S. Janβen, J. Phys. (France) II **4**, 837 (1994).
[25] A. Sariban and K. Binder, J. Chem. Phys. **86**, 5859 (1987).
[26] J. Bhattacharjee and R. A. Ferrell, Phys. Rev. A **23**, 1511 (1981).
[27] H. L. Swinney and D. L. Henry, Phys. Rev. A **8**, 2586 (1973).
[28] D. W. Oxtoby and W. M. Gelbart, J. Chem. Phys. **61**, 2957 (1974).
[29] K. Kawasaki and S. Lo, Phys. Rev. Lett. **29**, 48 (1972).
[30] P. C. Hohenberg and B. I. Halperin, Rev. Mod. Phys. **49**, 435 (1977).
[31] H. C. Burstyn, J. V. Sengers, J. K. Bhattacharjee, and R. A. Ferrell, Phys. Rev. A **28**, 1567 (1983).
[32] J. K. Bhattacharjee, R. A. Ferrell, R. S. Basu, and J. V. Sengers, Phys. Rev. A **24**, 1469 (1981).
[33] T. Ohta, J. Phys. C **10**, 791 (1977).
[34] M. E. Fisher, Phys. Rev. **176**, 257 (1968).
[35] L. D. Landau and E. M. Lifshitz, *Fluid Mechanics* (Pergamon, London, 1959).
[36] U. Genz and T. A. Vilgis, J. Chem. Phys. **101**, 7101 (1994).
[37] B. Steinhoff, L. Kühne, and I. Alig (unpublished).
[38] J. C. Le Guillou and J. Zinn-Justin, Phys. Rev. B **31**, 3976 (1980); C. Bervillier and C. Godreche, *ibid*. **21**, 5427 (1980).
[39] R. H. Beaumont, B. Clegg, C. Gee, J. B. M. Herbert, D. J. Marks, R. C. Roberts, and D. Sims, Polymer **7**, 401 (1966).